Sub-nanometer Pt Clusters Decoration Enhances the Oxygen Reduction Reaction Performances of NiOx Supported Pd Nano-islands

Authors: Dinesh Bhalothia,[a] Sheng Dai,[b,†] Sheng-Po Wang,[c] Che Yan,[a] Tzu-Hsi Huang,[d] Po-Chun Chen,[c] Nozomu Hiraoka,[d] Kuan-Wen Wang,[e*] and Tsan-Yao Chen[a,f*]

Affiliations:

[a.] Department of Engineering and System Science, National Tsing Hua University, Hsinchu 30013, Taiwan.

[b.] School of Chemistry & Molecular Engineering, East China University of Science and Technology, Shanghai 200237, P.R. China.

[c.] Department of Materials and Mineral Resources Engineering, National Taipei University of Technology, Taipei 10608, Taiwan.

[d.] National Synchrotron Radiation Research Center, Taiwan beamline office, SPring-8, 1-1-1 Koto, Sayo, Hyogo, 679-5198, Japan.

[e.] Institute of Materials Science and Engineering, National Central University, Taoyuan City 32001, Taiwan.

[f.] Hierarchical Green-Energy Materials (Hi-GEM) Research Centre, National Cheng Kung University, Tainan 70101, Taiwan.

[†] Dinesh Bhalothia and Sheng Dai have equal contribution to the first author

Corresponding Authors:

Tsan-Yao Chen

Email: chencaeser@gmail.com

Tel: +886-3-5715131 # 34271

FAX: +885-3-5720724

Kuan-Wen Wang

Email: kuanwen.wang@gmail.com

Tel: +886-3-4227151 # 34906

1. **HRTEM image of Ni@Pd NC.**

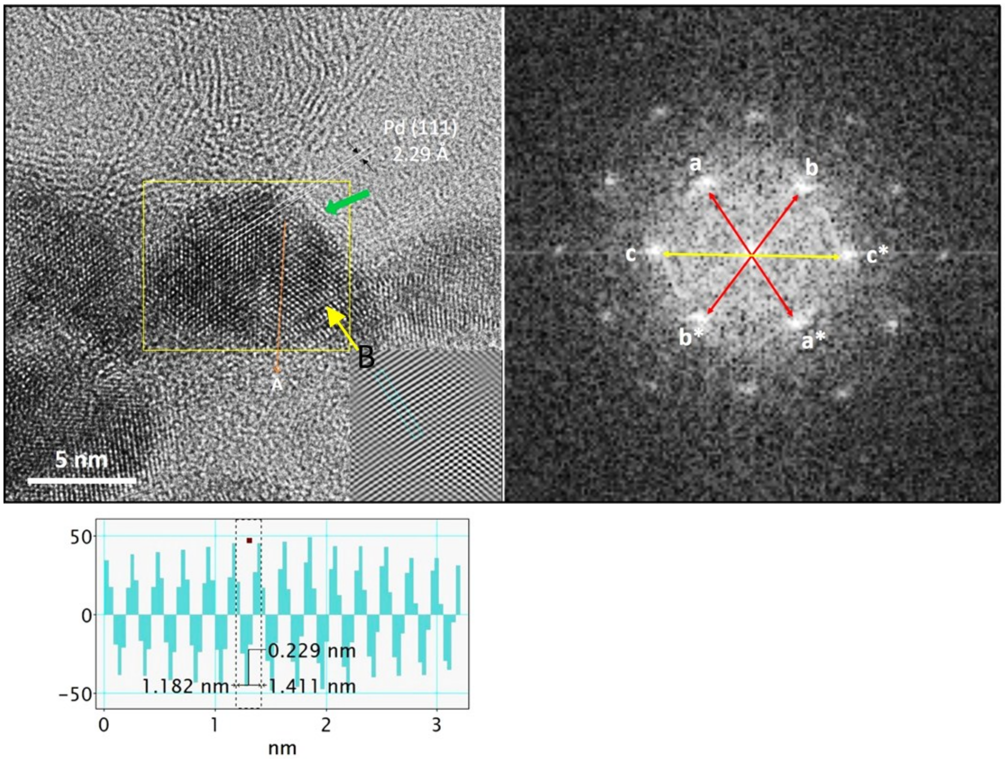

Figure S1. HRTEM image and IFT pattern of selected region for Ni@Pd (NP-1010) NC.

2. **XRD patterns of Pt-CNT, Pd-CNT, Ni-CNT, and Ni@Pd NCs.**

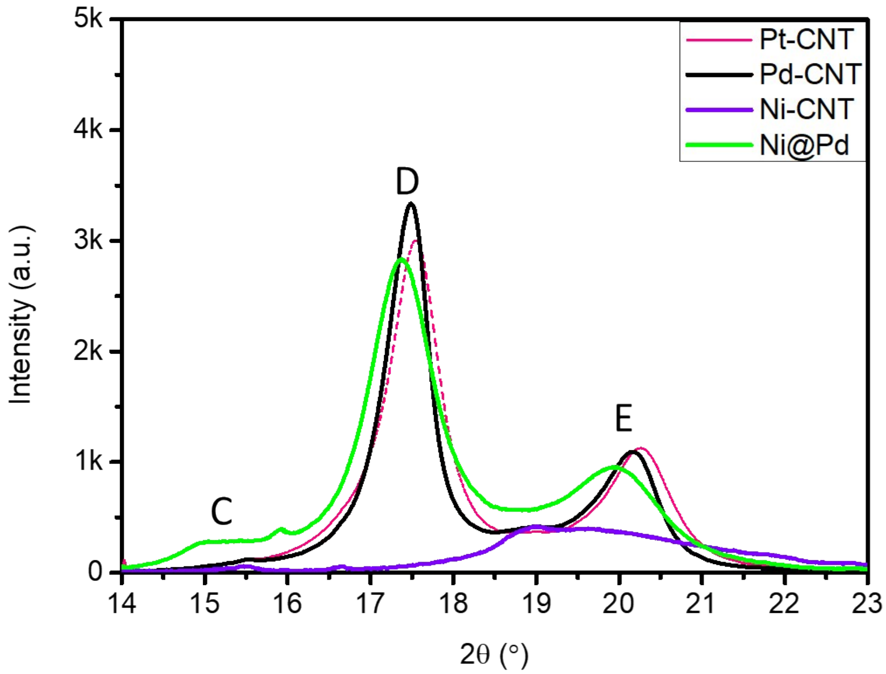

Figure S2. XRD patterns of Pt-CNT, Pd-CNT, Ni-CNT, and Ni@Pd NCs.

3. XRD determined structural parameters of experimental NPP NCs and control samples.

Table S1 XRD determined structural parameters of experimental NPP NCs and control samples.

NCs	d_{111} (Å)	d_{200} (Å)	d_{220} (Å)	$d_{(20\,-2\,-2)}$ (Å)	D_{111} (Å)	D_{200} (Å)	D_{220} (Å)	$D_{(20\,-2\,-2)}$ (Å)	h_{111}/h_{200}	h_{111}/h_{220}
Pd-CNT	2.270	1.965	1.389	NA	126.7	127.6	101.5	NA	3.01	6.39
Pt-CNT	2.262	1.961	1.382	NA	97.1	86.3	89.5	NA	2.65	4.75
Ni@Pd	2.277	1.986	1.398	1.536	37.0	26.1	23.9	69.1	2.97	5.46
NPP-01	2.262	1.980	1.386	1.528	77.1	46.5	57.5	61.9	2.72	5.54
NPP-02	2.264	1.971	1.388	1.526	92.4	65.8	63.4	49.0	2.73	5.93
NPP-03	2.261	1.977	1.388	1.528	71.6	54.5	60.7	60.0	2.93	5.87

d_{hkl} : interplanar spaccing

D_{hkl}: avergae grain

4. HRTEM image of Pt-CNT.

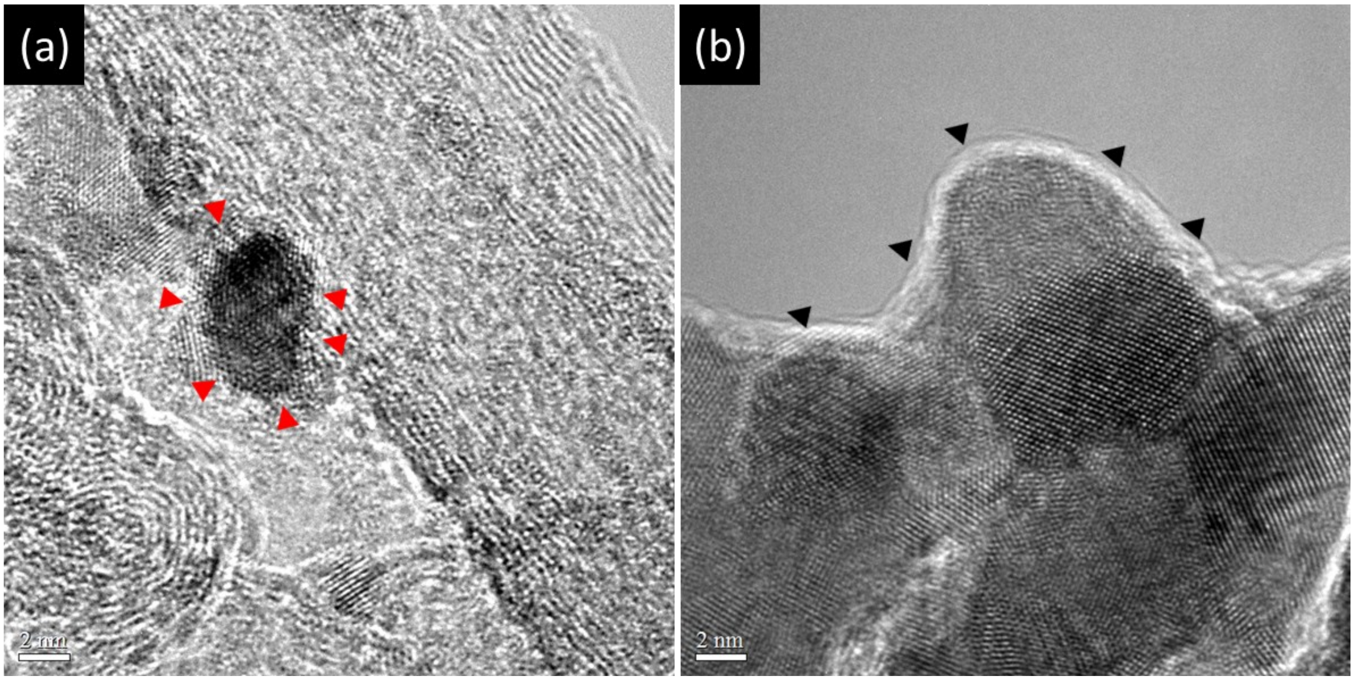

Figure S3. HRTEM image of (a) Pt-CNT where the terraces and surface truncation defects are denoted by red arrows. (b) Pd-CNT where agglomeration and surface rounding are denoted by black arrows.

5. Model analysis fitting curves compared with experimental FT-EXAFS spectra at Pt L_3-edge.

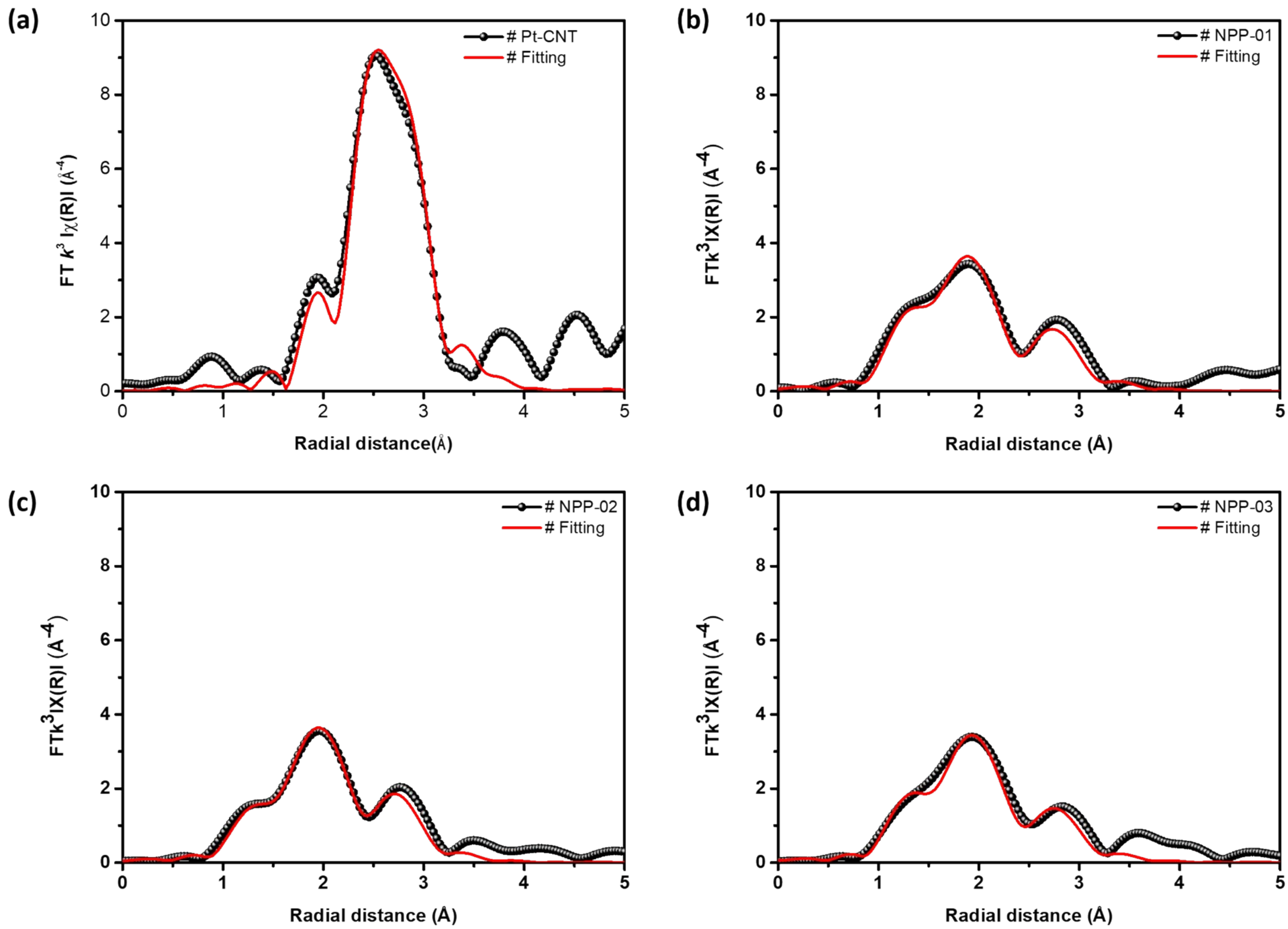

Figure S4. Model analysis fitting curves compared with experimental FT-EXAFS spectra at Pt L3-edge of (a) Pt-CNT, (b) NPP-01, (c) NPP-02 and (d) NPP-03.

6. X-ray absorption spectroscopy of NPP NCs and control samples at Pd k-edge.

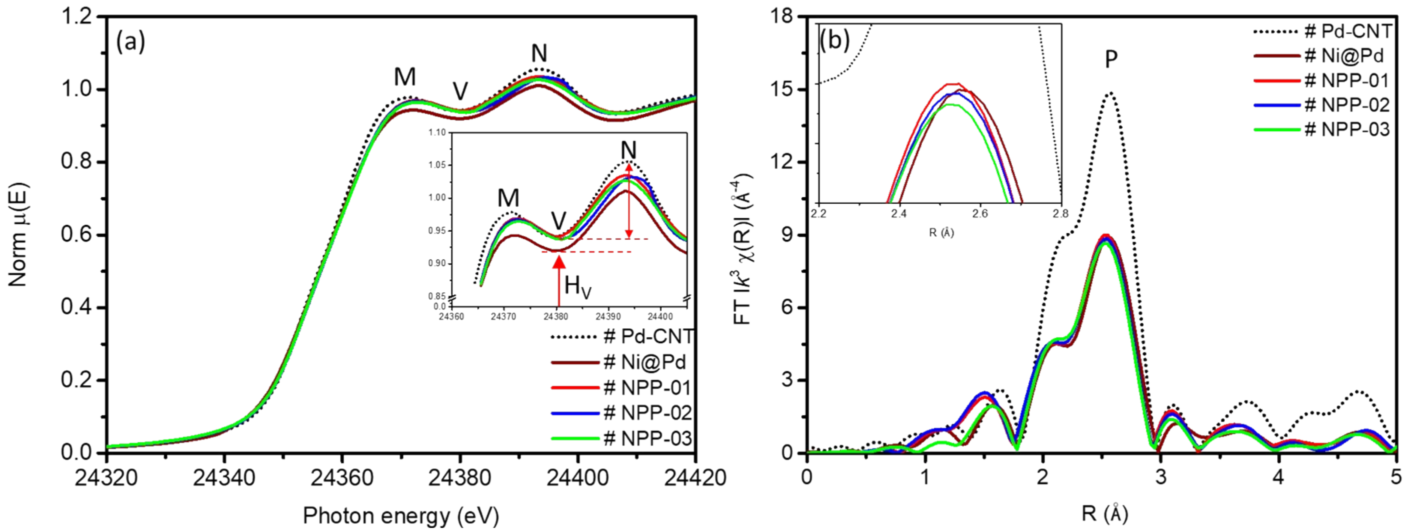

Figure S5 Pd K-edge X-ray absorption spectra of NPP NCs and Pd-CNT samples in (a) XANES and (b) Fourier transformed EXAFS regions.

7. Model analysis fitting curves compared with experimental FT-EXAFS spectra at Pd k-edge.

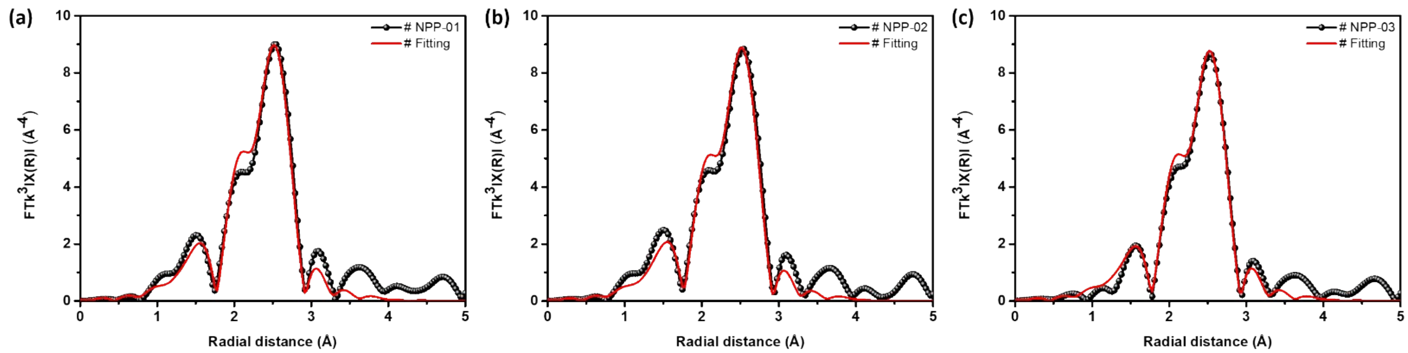

Figure S6. Model analysis fitting curves compared with experimental FT-EXAFS spectra at Pd k-edge of (a) NPP-01, (b) NPP-02 and (c) NPP-03.

8. X-ray absorption spectroscopy of NPP NCs and control samples at Ni k-edge.

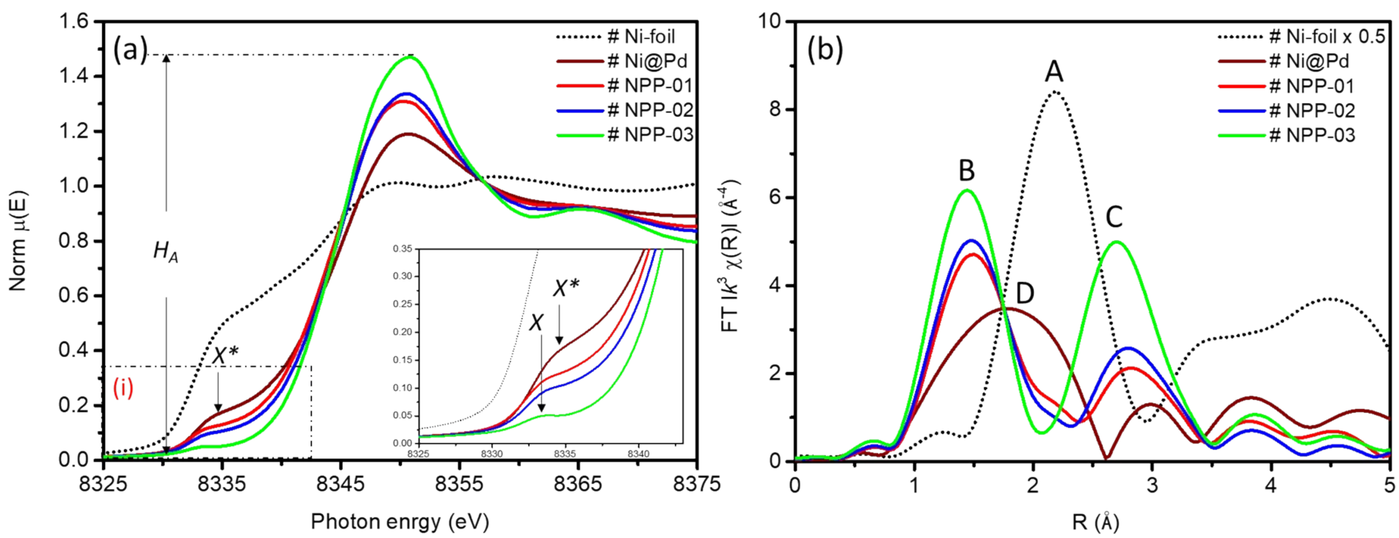

Figure S7. Ni K-edge X-ray absorption spectra of NPP NCs and Pd@Pd samples in (a) XANES and (b) Fourier transformed EXAFS regions.

9. X-ray photoemission spectroscopy (XPS) spectra of NPP NCs.

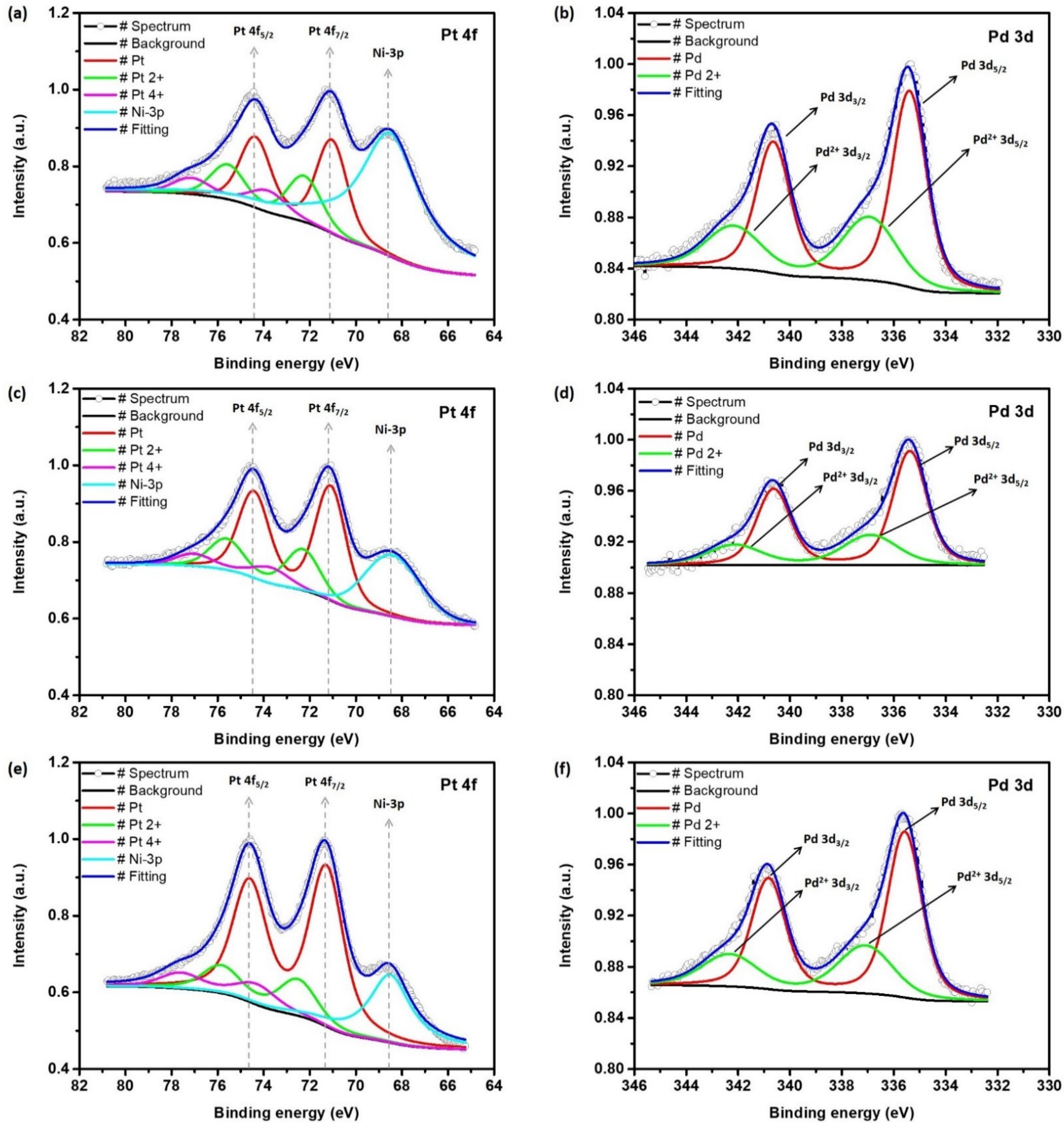

Figure S8. X-ray photoemission spectroscopy of NPP nanocatalysts. (a) Pt-4f/Ni-2p and (b) Pd 3d orbitals of NPP-01. (c) Pt-4f/Ni-2p and (d) Pd 3d orbitals of NPP-02. (e) Pt-4f/Ni-2p and (f) Pd 3d orbitals of NPP-03.

10. X-ray photoemission spectroscopy (XPS) spectra of control samples (Pd-CNT and Ni@Pd).

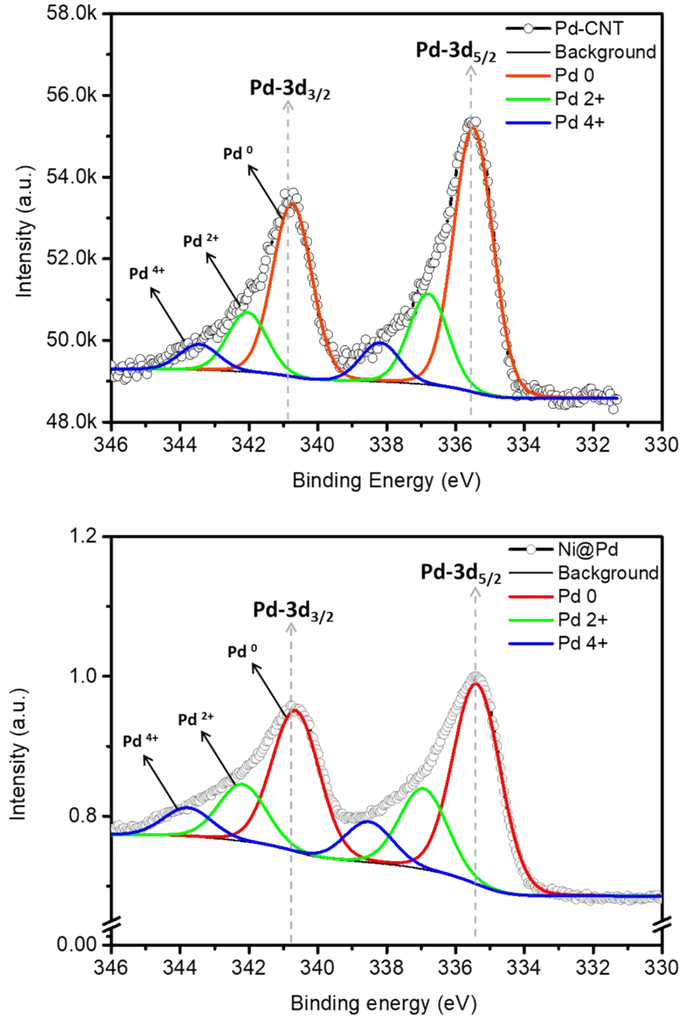

Figure S9. XPS spectrum and corresponding fitting curves of Pd-CNT and Ni@Pd in Pd 3d orbital

11. XPS fitting results of experimental NCs and control samples.

Table S2 XPS fitting results of experimental NCs and control samples.

<table>
<tr><th rowspan="2">Samples</th><th colspan="6">Elemental chemical states</th><th colspan="3">Composition (%)</th><th colspan="6">Binding Energy (eV)</th></tr>
<tr><th>Pt 0</th><th>Pt 2+</th><th>Pt 4+</th><th>Pd 0</th><th>Pd x+</th><th>NiOx</th><th>Pt</th><th>Pd</th><th>Ni</th><th>Pt 0</th><th>Pt 2+</th><th>Pt 4+</th><th>Pd 0</th><th>Pd 2+</th><th>NiOx</th></tr>
<tr><td>NPP-01</td><td>55.22</td><td>29.75</td><td>15.03</td><td>66.28</td><td>33.72</td><td>21.54</td><td>23.36</td><td>55.10</td><td>21.54</td><td>71.03</td><td>72.24</td><td>73.81</td><td>335.39</td><td>336.94</td><td>68.50</td></tr>
<tr><td>NPP-02</td><td>64.18</td><td>25.22</td><td>10.60</td><td>70.56</td><td>29.44</td><td>12.35</td><td>37.86</td><td>49.79</td><td>12.35</td><td>71.10</td><td>72.29</td><td>73.7</td><td>335.38</td><td>336.90</td><td>68.42</td></tr>
<tr><td>NPP-03</td><td>56.13</td><td>28.85</td><td>15.04</td><td>63.38</td><td>36.62</td><td>19.06</td><td>39.73</td><td>41.21</td><td>19.06</td><td>71.24</td><td>72.58</td><td>74.36</td><td>335.54</td><td>336.95</td><td>68.50</td></tr>
<tr><td>Ni@Pd</td><td colspan="3" rowspan="4">N/A</td><td>62.28</td><td>37.72</td><td colspan="4" rowspan="5">N/A</td><td colspan="3" rowspan="3">N/A</td><td>335.40</td><td>336.90</td><td rowspan="5">N/A</td></tr>
<tr><td>Pd-CNT</td><td>67.0</td><td>33.0</td><td>335.49</td><td>336.79</td></tr>
<tr><td>Pd-metal</td><td colspan="2" rowspan="3">N/A</td><td>335.60</td><td>N/A</td></tr>
<tr><td>Pt-metal</td><td>71.20</td><td colspan="4">N/A</td></tr>
<tr><td>J.M.-Pt/C</td><td>74.4</td><td>19.0</td><td>8.6</td><td>71.36</td><td>72.51</td><td>74.06</td><td colspan="2">N/A</td></tr>
</table>

12. CV and corresponding LSV curves of control samples including

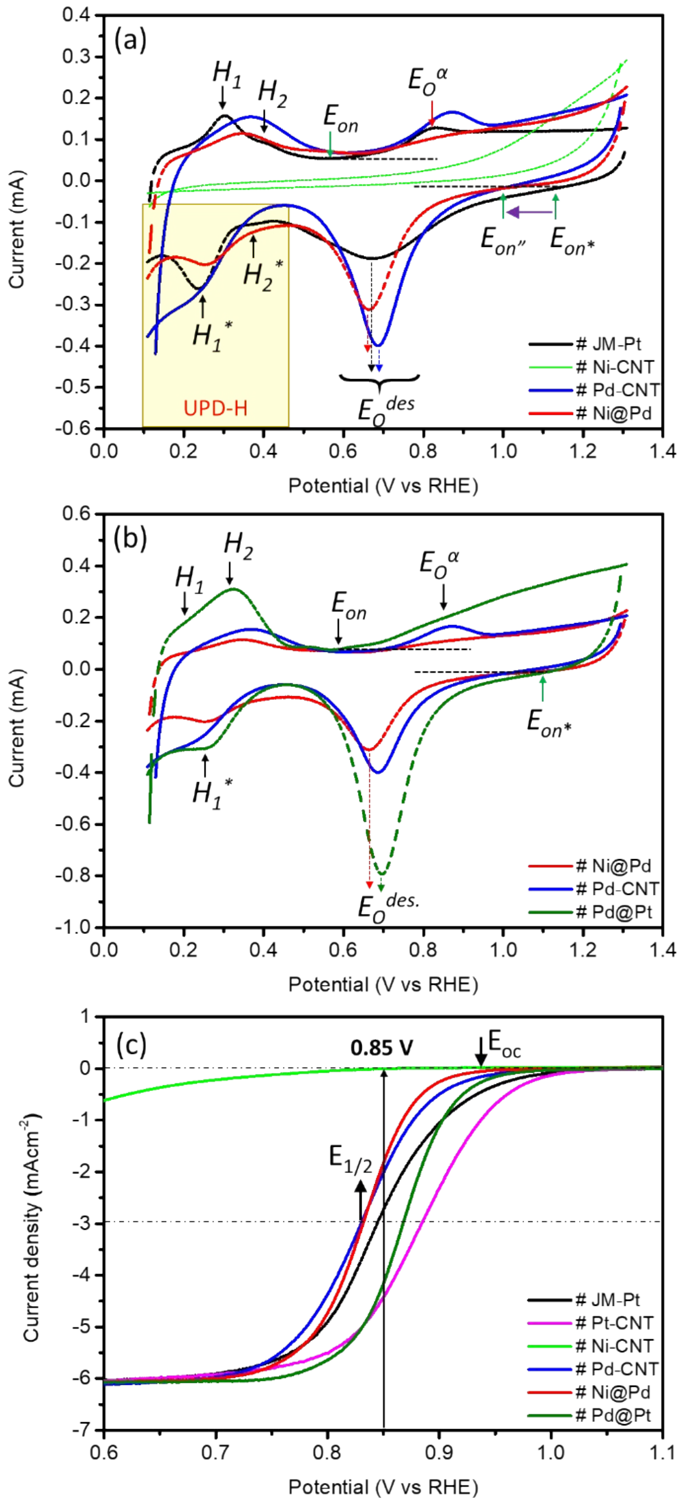

Figure S10. CV curves of control samples including (a) JM-Pt, Ni-CNT, Pd-CNT, Ni@Pd, (b) Ni@Pd, Pd-CNT, Pd@Pt, and (c) corresponding LSV curves of all control samples.

13. Electrochemical performances of NPP NCs compared with control sample and commercial Pt catalysts.

Table S3 Electrochemical performances of NPP NCs compared with control sample and commercial Pt catalysts (JM-Pt/C) at 0.85 V (vs. RHE) and 0.90 V (vs. RHE).

Sample	N(0.5V)	E_{oc} V vs RHE	$E_{1/2}$ V vs RHE	ESCA ($cm^2mg_{Pd+Pt}^{-1}$)	@ 0.85 V J_k $mAcm^{-2}$	@ 0.85 V M.A. ($mAmg_{Pt}^{-1}$)	@ 0.85 V M.A. ($mAmg_{Pd+Pt}^{-1}$)	@ 0.90 V J_k $mAcm^{-2}$	@ 0.90 V M.A. ($mAmg_{Pt}^{-1}$)	@ 0.90 V M.A. ($mAmg_{Pd+Pt}^{-1}$)
Ni-CNT		N/A				N/A				
Pd-CNT	4.0	0.895	0.831	555.1	2.33	N/A	41.6		N/A	
Pt-CNT	4.0	0.956		582.4	11.98	214.1	214.1			
Pd@Pt	4.0	0.915	0.867	961.9	10.33	1056.6	162.7			
Ni@Pd	3.9	0.881	0.832	206.4	2.09	N.A.	29.3	0.22	N.A.	3.1
NPP-01	3.4	0.940	0.885	285.4	10.85	872.0	135.1	2.39	191.8	29.7
NPP-02	3.7	0.990	0.932	248.2	36.06	1523.7	408.8	15.89	671.5	180.1
NPP-03	3.5	1.01	0.937	135.4	12.42	366.9	130.0	7.22	213.2	75.7
JM-Pt	4.0	0.910	0.844	257.0	4.37	67.0	67.0	1.21	24.9	24.9

* The E_{oc} is determined at a rotation speed of 1600 rpm with the value vs. RHE; N: Charge transfer number calculated at 0.5 V vs. RHE

14. Electrochemical impedance spectroscopy (EIS) spectra and fitting parameters of NPP NCs compared with control samples.

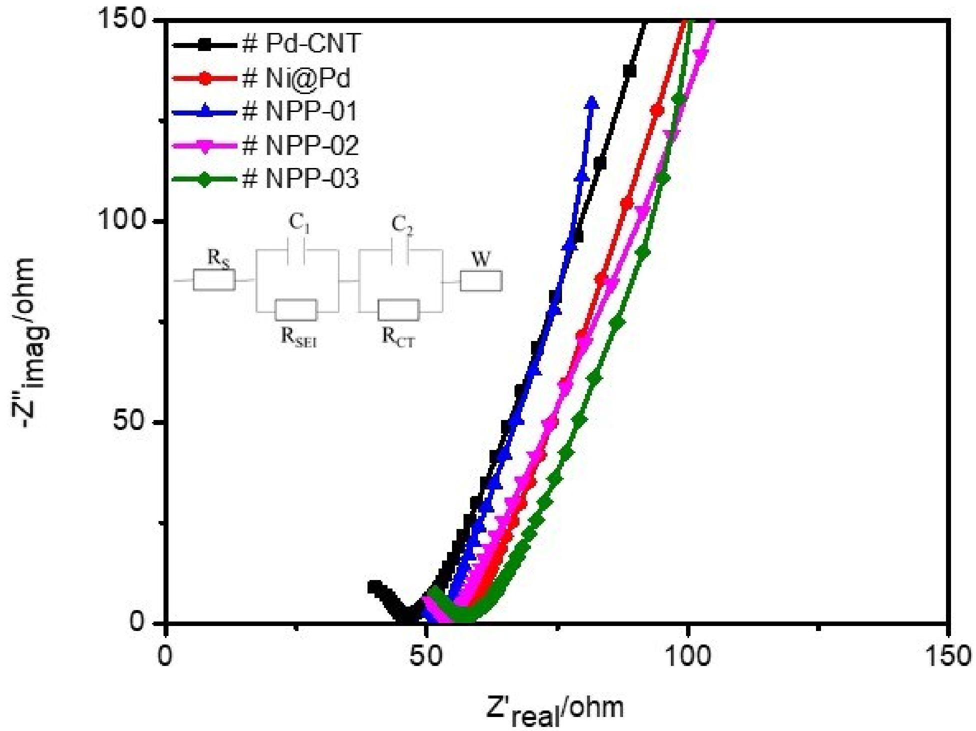

Figure S11. Electrochemical impedance spectroscopy (EIS) of NPP NCs compared with control samples.

Table S4. The electrochemical impedance parameters of NPP NCs and control samples.

Samples	R_S (W)	R_{CT} (W)	R_{SEI} (W)	R_W (W)
J.M.-Pt/C	45.20	5.31	2.04	8.26
Pd-CNT	42.15	7.26	2.15	7.96
Ni@Pd	37.95	16.73	2.24	9.69
NPP-01	44.69	8.06	0.92	4.38
NPP-02	41.63	11.12	1.93	8.06
NPP-03	39.38	16.02	2.95	6.22

15. CO stripping analysis for Pt cluster decoration effects on surface chemical environment of experimental NPP NCs

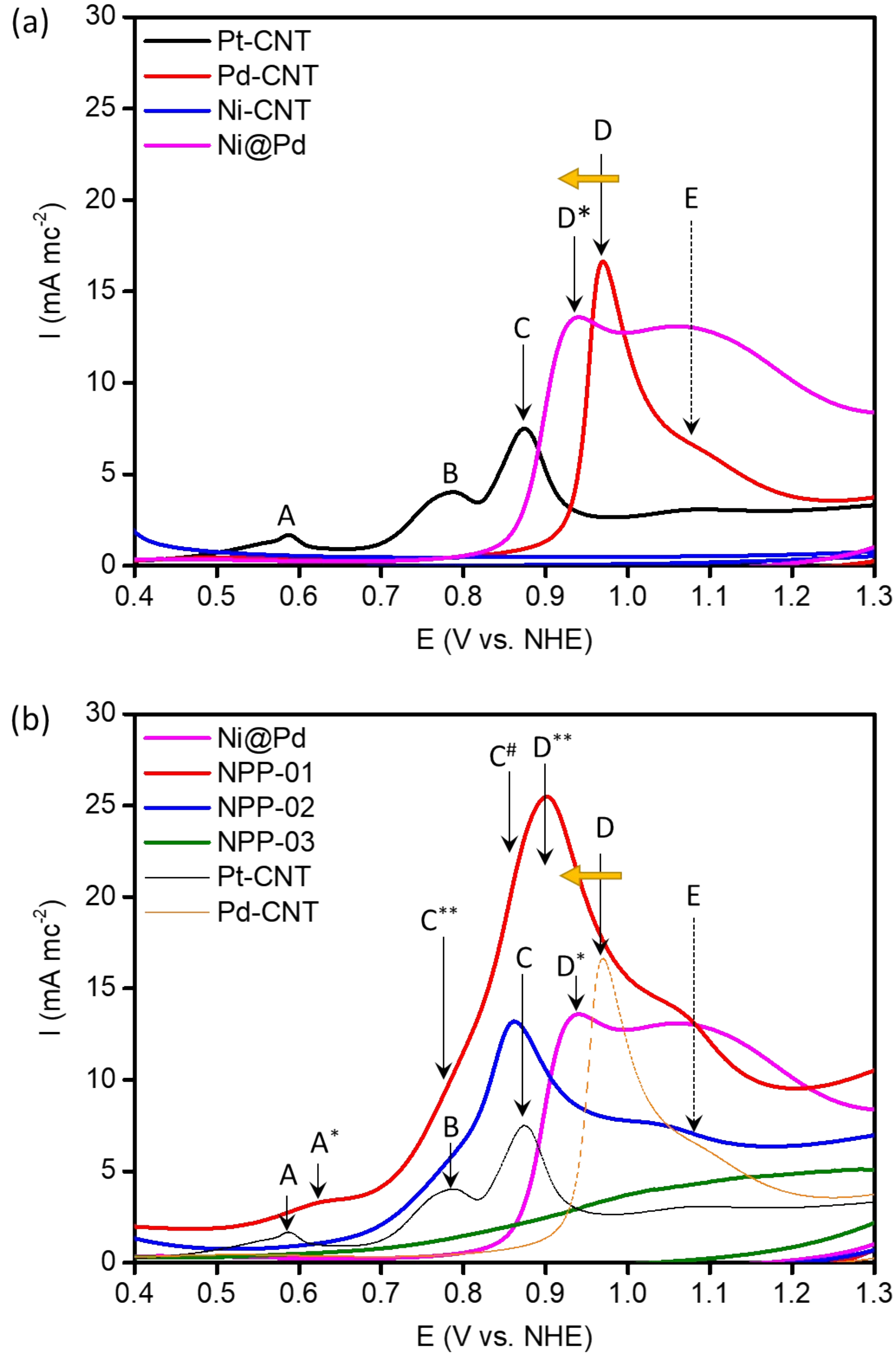

Figure S12. Co stripping curves of (a) control samples of Pt NPs, Pd NPs, Ni-CNT, and Ni@Pd NC; (b) control samples and experimental NPP NCs including NPP-01, NPP-02, and NPP-03.

16. Amount of H_2O_2 produced.

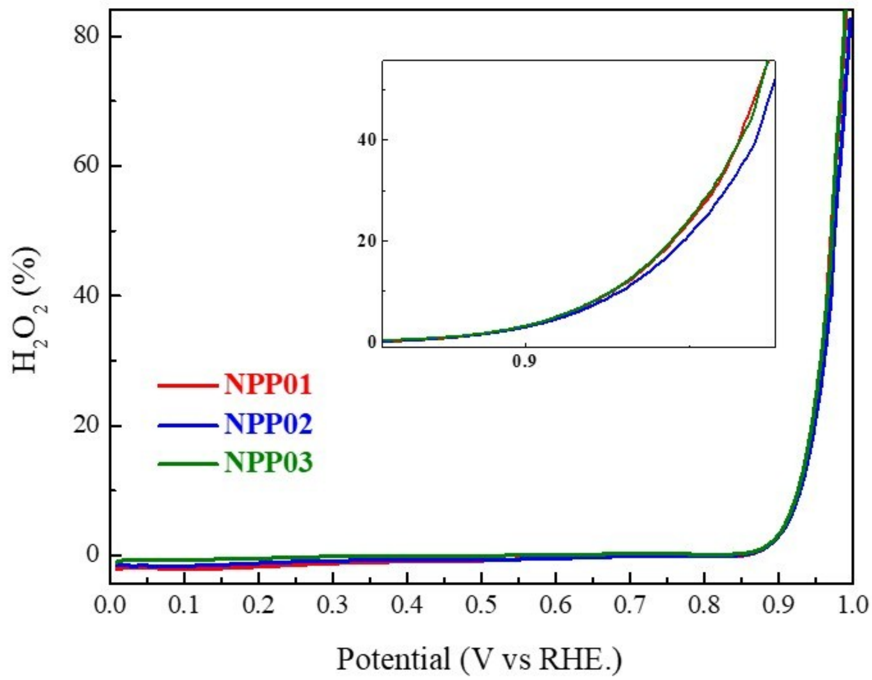

Figure S13. Amount of H_2O_2 produced during ORR.

Table S5. Amount of H_2O_2 produced during ORR with different experimental NCs.

Samples	**H_2O_2 (%) @0.85V (vs. RHE)**	**n**
NPP-01	0.22	3.9955
NPP-02	0.08	3.9984
NPP-03	0.28	3.9943

17. Accelerated degradation test (ADT) of experimental NCs.

Electrochemical stability of the NPP NCs was characterized using accelerated durability test (ADT) in potential range of 0.5V to 1.0V (V vs RHE.) with the applied scan rate of 0.05 Vs^{-1} in O_2 atmosphere for different ADT cycles.

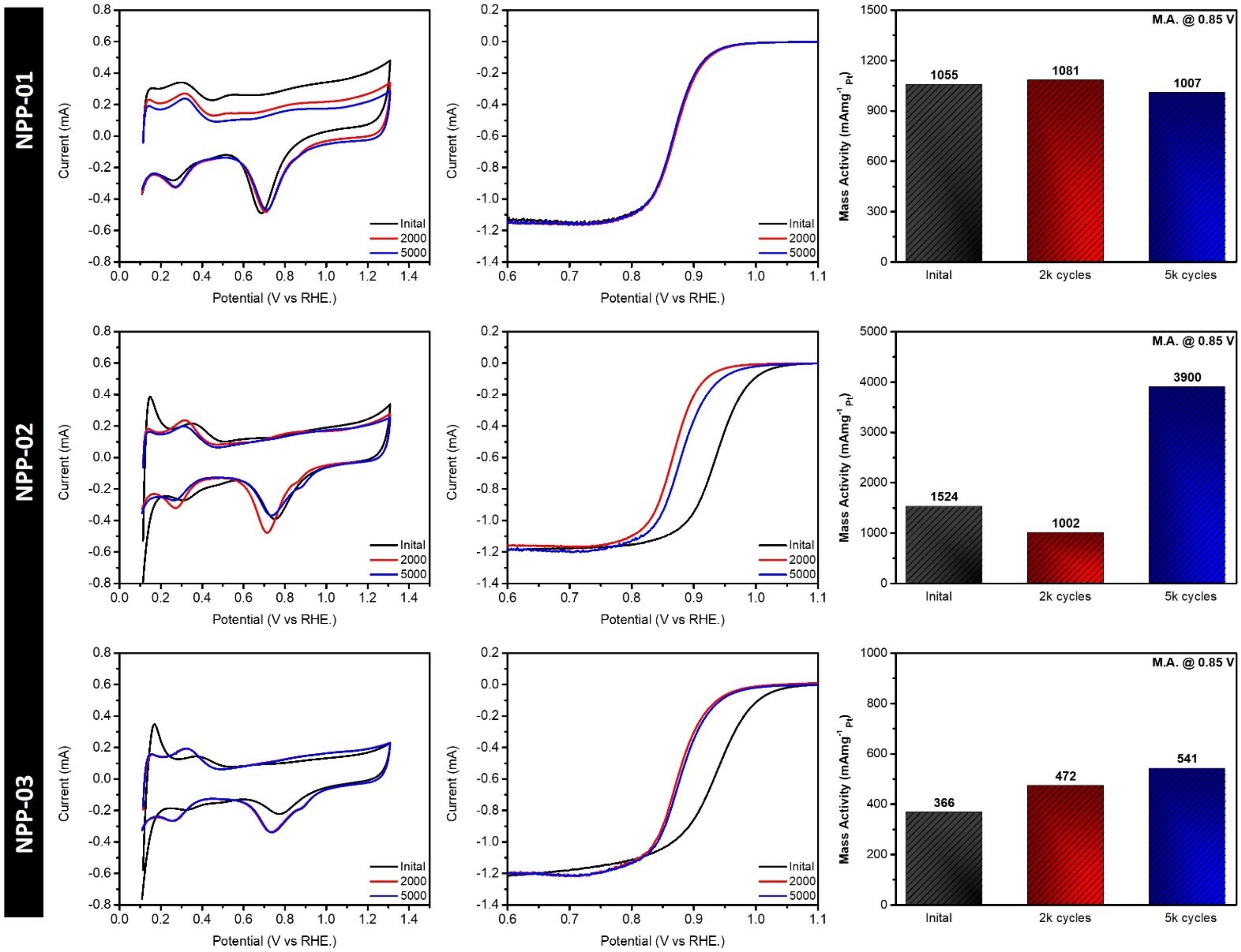

Figure S14. CV, LSV and corresponding MA of experimental NCs at different ADT cycles.

Table S6. Recent advances in Pt based heterogeneous catalysts for ORR

Catalysts	E_{onset} vs RHE	E_{half} vs RHE	MA total / Pt (mA / mg)	References
$Pt_{ML}/Pd/C$	NA	NA	240 @ 0.9V	Angew. Chem. Int. Ed. 2010, 49, 8602-8607
$Pt_{ML}/Pd_9Au_1/C$	NA	NA	300 @ 0.9V	Angew. Chem. Int. Ed. 2010, 49, 8602-8607
Co@Pt-NC framework	NA	NA	71.9 @ 0.85 V	Journal of Power Sources 343 (2017) 458e466
$PdCu_2$@Pt-H	NA	NA	485	Applied catalysis B: Environmental 225(2018) 84-90

Pd2@PtNi/MWCNT	NA	NA	73.3	Journal of Power Sources 365 (2017) 26e33
Pt@Pd	0.97	0.88	NA	J. Power Sources 2014, 268, 712−717
Cu@Pd/Pt	0.909	NA	414	Nanoscale, 2017, 9, 7207
H-Pt/CaMnO3	0.95	0.81	380 @ 0.85V	J. Adv. Mater. 2014, 26, 2047−2051
Pt@Au/PyNG	0.92	NA	NA	ACS Appl. Mater. Interfaces 2014, 6, 13448−13454
Pt-N/C PMC	NA	NA	162.88 ($mAug^{-1}$)	Carbon 128 (2018) 38-45
40 wt.% Pt/BC	NA	NA	209 @ 0.9V	Nature Communications volume8, Article number: 15802 (2017)
PtPd NRs	NA	NA	580 @ 0.9V	Adv. Mater. 2018, 30, 1802136